Received May 1, 2020, accepted May 12, 2020, date of publication May 14, 2020, date of current version May 28, 2020.

Digital Object Identifier 10.1109/ACCESS.2020.2994653

Power Stability Optimization Design of Three-Dimensional Wireless Power Transmission System in Multi-Load Application Scenarios

LINLIN TAN[1,2], RUYING ZHONG[1], ZONGYAO TANG[1], TIANYI HUANG[1], XUELIANG HUANG[1,2], (Member, IEEE), TAO MENG[1], XUEFENG ZHAI[3], CHENGLIANG WANG[3], YAN XU[3], AND QINGSHENG YANG[3]

[1]School of Electrical Engineering, Southeast University, Nanjing 210096, China
[2]Key Laboratory of Smart Grid Technology and Equipment in Jiangsu Province, Zhenjiang 212000, China
[3]Jiangsu Fangtian Technology Company., Ltd., Nanjing 211100, China

Corresponding author: Linlin Tan (tanlinlin@seu.edu.cn)

This work was supported in part by the National Natural Science Foundation of China under Grant 51877036, in part by the Southeast University's Zhishan Young Scholar Support Program, and in part by the Fundamental Research Funds for the Central Universities.

ABSTRACT Recently, most wireless power transmission (WPT) systems have used a ''one-to-one'' charging method of one receiving coil to one transmitting coil. However, when the receiving coil is offset in this way, the mutual inductance between the transmitting and receiving coils will be weakened, and the flexibility of the WPT system application will also be reduced. Therefore, how to realize the ''one-to-many'' transmission mode of one transmitting coil to multiple receiving coils and ensure the power stability of multiple loads is an urgent problem to be solved. In order to solve the above problems, the LCC-S topology is combined with the three-phase circuit, and a three-phase omnidirectional WPT system coil scheme is proposed based on the power characteristics of the three-phase LCC-S topology in this paper. Firstly, the influence of the resonance compensation topology on power characteristics is analyzed through circuit theory and a more suitable LCC-S topology is chosen. Then, the optimal coil scheme of the three-phase omnidirectional WPT system is proposed based on the law of mutual inductance. Compared with the original scheme, the theoretical calculation results show that the power fluctuation of the system is reduced by 75.13%. Finally, a set of three-phase WPT system model and test systems similar to the theory are established, which effectively verify the improvement of the proposed scheme, and verify the correctness and feasibility of the scheme.

INDEX TERMS Wireless power transfer, multi-load power transmission, three-phase omnidirectional wireless power transmission system, coil design, LCC-S topology, power stabilization.

I. INTRODUCTION

As a novel charging technology, wireless power transmission (WPT) technology has the characteristics of simple charging process and simplified charging facilities. In recent years, WPT technology has developed rapidly and has been widely used in electric vehicles, mobile phones, implantable medical devices and other fields [1]–[4]. However, most of the wireless charging systems used ''one-to-one'' charging mode, and when the receiving coil is shifted horizontally, vertically, or angularly, the mutual inductance between the transmitting and receiving coils will be weakened correspondingly, thereby reducing the transmission performance of the system. In addition, the ''one-to-one'' charging mode also limits the flexibility of WPT system application to a large extent and is not conducive to the efficient use of resources. Therefore, it is an urgent issue to realize the ''one-to-many'' transmission of power and ensure the stability of the load power in the system when the load is accessed or removed.

Literature [5] took S-S topology as the analysis object, and considered all the load coils in a multi-load system as relay coils. By optimizing the matching of system parameters, multiple loads at different distances could receive the same power. However, when the quantity changes, it is still necessary to re-match the information parameters. Literature [6] proposed a dynamic control method using impedance matching through

The associate editor coordinating the review of this manuscript and approving it for publication was Meng Huang.

the analysis of S-S topology to solve the problem of power fluctuation in multi-load scenarios. Literature [7] proposed the use of impedance matching network to adjust the value of each load by analyzing the characteristics of the multi-load wireless charging system to meet certain constraints to solve the power fluctuation problem. Literature [8] adopts the method of frequency tracking and continuously adjusts the resonance capacitance in the system to ensure the stability of the received power of each load when the number of loads changes. However, most of the methods described so far require additional control methods, which increases the cost of the system and the complexity of the application to a certain extent. Therefore, the current power stability problem still needs new solutions.

In order to solve the above problem, in recent years, some scholars have proposed to generate a rotating magnetic field around the transmitting coil to ensure that the receiving coil can receive power at any angle of the transmitting coil, which is called the omnidirectional WPT technology. In the past studies, the research on omnidirectional WPT technology is mainly divided into two aspects: one is to optimize the performance of omnidirectional WPT system by improving the circuit control strategy and circuit topology; the other is to improve the coil scheme of various omnidirectional WPT systems to achieve more functions.

In terms of circuit control strategies and circuit topology research, literature [9] proposed a non-identical current control method for 2-D and 3-D omnidirectional WPT system. By controlling the amplitude of the current source, the circuit current was controlled to generate a rotating magnetic field satisfying the requirements. Literature [10] and [11] performed mathematical analysis on 2-D and 3-D omnidirectional WPT systems respectively, proving the consistency of maximum transmission efficiency and maximum load power direction in geometric space, and effectively guiding power to the load by controlling the input magnetic vector angle. Based on the basic principle of current amplitude control, literature [12] reduced the unnecessary transfer of power to the no-load region and improved the system efficiency through directional power flow control. Literature [13], [14] proposed a three-phase wireless power transmission system based on the S-S resonance compensation topology. The zero-voltage switch was realized through parameter optimization, and the stable power output of the system was guaranteed within the whole angle misalignment range. However, the circuit topology and control strategies of the omnidirectional WPT system proposed in the above literatures are mainly based on the S-S resonance compensation topology and current source input, which is not easy to design and implement in practical applications. Moreover, the proposed directional power control is mainly applicable to single load or concentrated load situation, while the problem of insufficient power supply and power fluctuation may occur when loads are numerous and dispersed. Therefore, considering the above problems, this paper combines the LCC-S resonance compensation topology with the three-phase circuit and applies it to a multi-load scenario, so a three-phase LCC-S compensation topology under multi-load is proposed. Through circuit analysis, the problem of power drop or sudden rise when the load is accessed or removed under the S-S topology is solved.

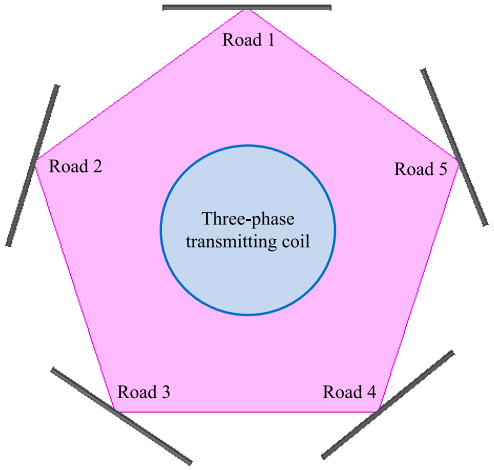

FIGURE 1. Top view of load distribution in omnidirectional WPT system.

In terms of omnidirectional WPT coil design, literature [15] and [16] proposed an omnidirectional WPT system with a new cubic transmitter, which achieved relatively high transmission efficiency. As the original omnidirectional WPT system, its power transmission in some special locations would drop significantly. Based on the omnidirectional WPT coil model above, literature [17] and [18] proposed an orthogonal receiving coil composed of three sets of coils, which improved the potential of the angular offset sensitivity of the omnidirectional WPT system. However, each of its three sets of coils requires an AC current source, which is cumbersome and expensive to implement. Therefore, to solve the problems of the coil solutions in the above literature, this paper combines their coil advantages, and proposes a three-phase omnidirectional WPT system coil solution in a multi-load application scenario, which reduces the power fluctuation under the deviation of multi-load. Moreover, only one voltage source is needed as the power source, which improves the feasibility of actual implementation and reduces costs.

In summary, this paper combines LCC-S resonance compensation topology with a three-phase circuit to propose a three-phase LCC-S compensation topology under multiple loads firstly. Then considering the multi-load application scenario, a three-phase omnidirectional WPT system coil scheme is proposed in the multi-load application scenario. The contribution of this article is to propose the new idea of applying LCC-S topology in three-phase circuit for the first time, and then to propose a method of winding orthogonal three-dimensional coils combined with three-phase circuits. This three-phase LCC-S circuit combined with a quadrature coil winding method can not only solve the power drop or sudden increase when the load is connected or removed, reduce the power fluctuations that occur

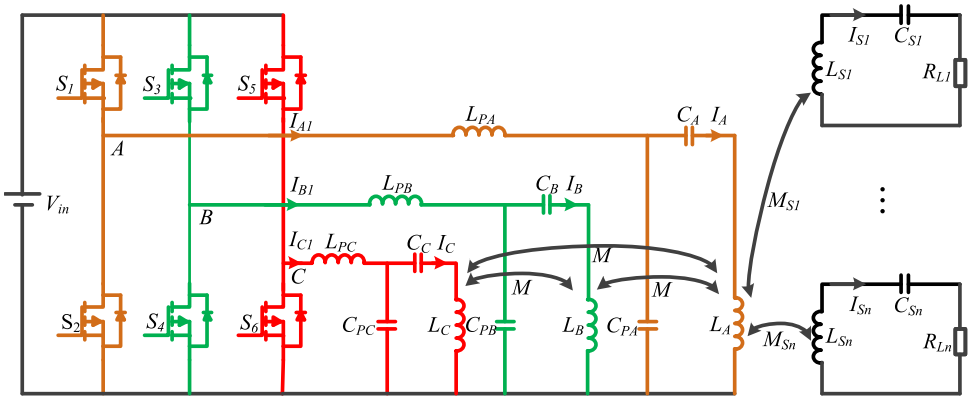

FIGURE 2. Overall structure of three-phase WPT system.

when the load angle is shifted, and improve the transmission power stability. Besides, it can also reduce the number of power supplies and reduce power costs. The rest of the paper is arranged as follows. Section II compares and analyzes the compensation topology in the multi-load application scenario. Section III optimizes the design of the spatial orthogonal three-phase coil based on the three-phase LCC-S topology in the multi-load coil application scenario. Section IV is the experimental verification. Section V is the conclusion.

II. SYSTEM TOPOLOGY ANALYSIS IN MULTI-LOAD APPLICATION SCENARIOS

The omnidirectional WPT systems mentioned in the current literature mainly include two types: (1) Omnidirectional WPT system for directional power transmission based on load position [19], [20]. (2) Constant transmission power in the space [21], [22]. Although the directional transmission power according to the load position can effectively improve the transmission efficiency of the system in a multi-load application scenario, complex control is required to achieve multi-load positioning and power directional transmission. Therefore, the former system is more suitable for an omnidirectional WPT system with a small number of loads or the relatively concentrated loads, while the latter system is more suitable for an omnidirectional WPT system with a large number of loads and a relatively uniform distribution. This paper will focus on the latter system, and assume that the load is evenly distributed around the transmitting coil and is facing the center of the circle. The top view of the system distribution when the number of loads is five is shown in Fig.1.

The overall structure of the three-phase WPT system is shown in Fig.2. Its working principle is as follows: The DC power source inverts the DC voltage into three-phase high-frequency AC power through a three-phase inverter, which is fed into the transmitting coil through the resonance compensation network to generate high-frequency electromagnetic field. The receiving coil on the load side obtains energy by means of magnetic field coupling, thereby achieving wireless power transmission. The output voltage of the three-phase inverter can change the phase between $\dot{U}_A$, $\dot{U}_B$ and $\dot{U}_C$ by adjusting the phase between the input PWM waves in the MOSFET. $\dot{U}_A$, $\dot{U}_B$ and $\dot{U}_C$ can be written as

$$\begin{cases} \dot{U}_A = U\angle 0° \\ \dot{U}_B = U\angle \alpha \\ \dot{U}_C = U\angle \beta \end{cases} \tag{1}$$

In Fig.2, S_1~S_6 represent the switching tubes of three-phase bridge inverter circuit. L_{PA}, L_{PB} and L_{PC} represent the primary side compensation inductors for phases A, B and C respectively. and L_A, L_B, L_C and L_{Sn} represent the inductors of the transmitting coils for phases A, B, C and receiving coil respectively. C_{PA}, C_{PB} and C_{PC} denote the primary side compensation capacitors for phases A, B and C respectively, and C_A, C_BC_C and C_{Sn} denote the capacitors of the transmitting coils for phase A, B, C and receiving coil. M represents mutual inductance between the coils of phase A, B and C.M_{An}, M_{Bn} and M_{Cn} (n=1, 2, ...) represent the mutual inductance between the transmitting coils of phase A, B, C and the n^{th} receiving coil. $\dot{I}_A$, $\dot{I}_B$, $\dot{I}_C$ and $\dot{I}_{Sn}$ (n=1, 2, ...) represent the currents flowing through the phase A, B, C and the n^{th} load respectively, and R_{Ln} represents the equivalent resistance of the n^{th} load.

A. TRADITIONAL THREE-PHASE S-S COMPENSATION TOPOLOGY FOR MULTI-LOAD RECEIVING SYSTEMS

Literature [23] used a three-phase S-S topology to analyze the transmission characteristics of a WPT system under a single load and optimize the parameters to realize soft switching technology. In order to compare with the proposed three-phase LCC-S topology, the theoretical and simulation analysis of the traditional three-phase S-S compensation topology is performed in this section.

The three-phase S-S compensation topology for a multi-load receiving system is shown in Fig.3. The meaning of the letter symbols in Fig.3 is the same as that of the same letter symbols in Fig.2. To simplify the analysis, we assume $R_{L1} = R_{L2} = \ldots = R_{Ln} = R_L$. In addition, considering that the reactance of the coil is much larger than the internal resistance

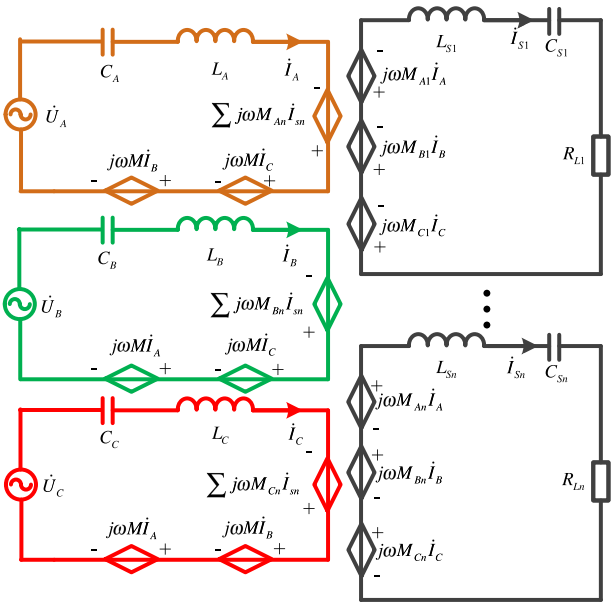

FIGURE 3. Mutual inductance equivalent model of three-phase S-S compensation topology.

of the coil, the influence of the internal resistance of the coil can be ignored in the analysis. Moreover, considering that the influence of cross coupling can be eliminated by means of reactance compensation, the influence of cross coupling is not considered here [24].

To ensure that the system is in resonance, the following relationships need to be satisfied:

$$\begin{aligned}\omega &= \frac{1}{\sqrt{L_A C_A}} = \frac{1}{\sqrt{L_B C_B}} = \frac{1}{\sqrt{L_C C_C}} \\ &= \frac{1}{\sqrt{L_{S1} C_{S1}}} = \cdots = \frac{1}{\sqrt{L_{Sn} C_{Sn}}}\end{aligned} \tag{2}$$

According to Fig.3, the KVL equation can be written as

$$\begin{bmatrix}\dot{U}_A\\ \dot{U}_B\\ \dot{U}_C\end{bmatrix} = \begin{bmatrix}0 & j\omega M & j\omega M\\ j\omega M & 0 & j\omega M\\ j\omega M & j\omega M & 0\end{bmatrix}\begin{bmatrix}\dot{I}_A\\ \dot{I}_B\\ \dot{I}_C\end{bmatrix} - \begin{bmatrix}j\omega M_{A1} & j\omega M_{A2} & \cdots & j\omega M_{An}\\ j\omega M_{B1} & j\omega M_{B2} & \cdots & j\omega M_{Bn}\\ j\omega M_{C1} & j\omega M_{C2} & \cdots & j\omega M_{Cn}\end{bmatrix}\begin{bmatrix}\dot{I}_{S1}\\ \dot{I}_{S2}\\ \vdots\\ \dot{I}_{Sn}\end{bmatrix} \tag{3}$$

$$\begin{bmatrix}0\\ 0\\ \vdots\\ 0\end{bmatrix} = \begin{bmatrix}j\omega M_{A1} & j\omega M_{B1} & j\omega M_{C1}\\ j\omega M_{A1} & j\omega M_{B1} & j\omega M_{C1}\\ \vdots & \vdots & \vdots\\ j\omega M_{An} & j\omega M_{Bn} & j\omega M_{Cn}\end{bmatrix}\begin{bmatrix}\dot{I}_A\\ \dot{I}_B\\ \dot{I}_C\end{bmatrix} + \begin{bmatrix}R_L & 0 & \cdots & 0\\ 0 & R_L & \cdots & 0\\ \vdots & \vdots & \ddots & \vdots\\ 0 & 0 & 0 & R_L\end{bmatrix}\begin{bmatrix}\dot{I}_{S1}\\ \dot{I}_{S2}\\ \vdots\\ \dot{I}_{Sn}\end{bmatrix} \tag{4}$$

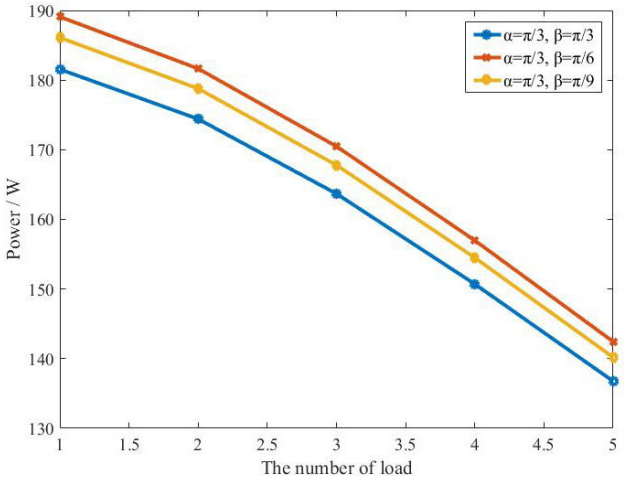

FIGURE 4. Theload received power influenced by load quantity in three-phase S-S resonance compensation topology.

To simplify equations (3) and (4), we use:

$$U = \begin{bmatrix}\dot{U}_A & \dot{U}_B & \dot{U}_C\end{bmatrix}^T \tag{5}$$

$$A = \begin{bmatrix}0 & j\omega M & j\omega M\\ j\omega M & 0 & j\omega M\\ j\omega M & j\omega M & 0\end{bmatrix} \tag{6}$$

$$I = \begin{bmatrix}\dot{I}_A & \dot{I}_B & \dot{I}_C\end{bmatrix}^T \tag{7}$$

$$B = \begin{bmatrix}j\omega M_{A1} & j\omega M_{A2} & \cdots & j\omega M_{An}\\ j\omega M_{B1} & j\omega M_{B2} & \cdots & j\omega M_{Bn}\\ j\omega M_{C1} & j\omega M_{C2} & \cdots & j\omega M_{Cn}\end{bmatrix} \tag{8}$$

$$I_S = \begin{bmatrix}\dot{I}_{S1} & \dot{I}_{S2} & \cdots & \dot{I}_{Sn}\end{bmatrix}^T \tag{9}$$

$$R = \begin{bmatrix}R_L & 0 & \cdots & 0\\ 0 & R_L & \cdots & 0\\ 0 & 0 & \cdots & R_L\end{bmatrix} \tag{10}$$

Then

$$U = AI - BI_S \tag{11}$$

$$0 = B^T I - RI_S \tag{12}$$

Therefore, it can be solved as

$$I = \left(A - BR^{-1}B^T\right)^{-1} U \tag{13}$$

$$I_S = R^{-1}B^T\left(A - BR^{-1}B^T\right)^{-1} U \tag{14}$$

So, the power received by the n^{th} load is

$$P_{out\_n} = Re(R_L \cdot \dot{I}_{Sn} \cdot \dot{I}_{Sn}^*) \tag{15}$$

According to (15), the trend of the received power of each load varying with the number of loads can be calculated and plotted as shown in Fig.4. Since the transmitting coil will be optimized later to ensure that the sum of the mutual inductance of the receiving coil at each position is basically the same, it is assumed here that the mutual inductance between the load and the transmitting coil is the same.

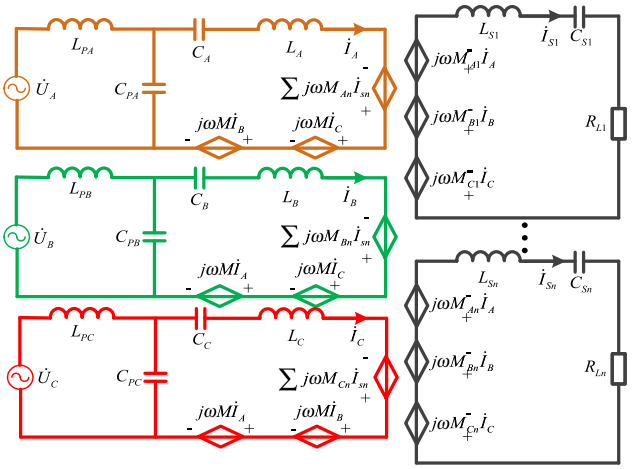

FIGURE 5. Mutual inductance equivalent model of three-phase LCC-S compensation topology.

It can be seen from Fig.4 that under the three-phase S-S resonance compensation topology, the power received by each load gradually decreases with the increase of the number of loads, and under different input voltage phase angles, the downward trend of load receiving power remains basically the same. This is because when the number of loads increases, the equivalent resistance from the receiving terminal to the transmitting terminal increases, so the current value flowing through the transmitting coil decreases, resulting in a decrease in the induced voltage in the receiving coil. According to the power calculation formula $P=U^2/R_L$, the received power of the load will decrease as the number of loads increases. Therefore, under the three-phase S-S resonance compensation topology, the receiving power of the load that is being charged will be affected by the insertion or removal of other loads, which will cause the receiving power of the load to drop or rise sharply and eventually cause equipment and battery aging and damage.

B. THREE-PHASE LCC-S COMPENSATION TOPOLOGY FOR MULTI-LOAD RECEIVING SYSTEMS

According to part A, the received power of the load in the three-phase S-S resonance compensation topology is affected by the insertion or removal of other loads. In order to solve the above problem, this paper proposes a three-phase LCC-S resonance compensation topology, and its mutual inductance equivalent model is shown in Fig.5.

The meaning of the letter symbols in Fig.5 is the same as the meaning of the same letter symbols in Fig.2. Similarly, in order to simplify the analysis, we suppose $R_{L1} = R_{L2} = \ldots = R_{Ln} = R_L$ and $L_{PA} = L_{PB} = L_{PC} = L_P$. In addition, considering that the reactance of the coil is much larger than the internal resistance of the coil, the influence of the internal resistance of the coil can be ignored in the power analysis.

To ensure that the system is in resonance, the system parameters meet:

$$\begin{cases} L_{PA}C_{PA} = L_{PB}C_{PB} = L_{PC}C_{PC} = 1/\omega^2 \\ C_A(L_A - L_{PA}) = C_B(L_B - L_{PB}) \\ \quad = C_C(L_C - L_{PC}) = 1/\omega^2 \\ L_{S1}C_{S1} = \cdots = L_{Sn}C_{Sn} = 1/\omega^2 \end{cases} \tag{16}$$

According to [25], it can be seen that the characteristics of the constant current source are located at the transmitting coil of the LCC resonance compensation topology. So it can be obtained as

$$\begin{cases} \dot{I}_A = \dot{U}_A/(j\omega L_P) \\ \dot{I}_B = \dot{U}_B/(j\omega L_P) \\ \dot{I}_C = \dot{U}_C/(j\omega L_P) \end{cases} \tag{17}$$

According to Fig.5, the KVL equation can be written as, (18), as shown at the bottom of the next page.

The current flowing through the n[th] load is calculated as

$$\dot{I}_{Sn} = \frac{M_{An}\dot{U}_A + M_{Bn}\dot{U}_B + M_{Cn}\dot{U}_C}{L_P R_L} \tag{19}$$

The received power of the n[th] load is

$$\begin{aligned} &P_{out\_n} \\ &= Re(R_L \cdot \dot{I}_{Sn} \cdot \dot{I}_{Sn}^*) \\ &= \frac{U^2}{L_P^2 R_L} \cdot |M_{An} + M_{Bn}\angle\alpha + M_{Cn}\angle\beta|^2 \\ &= \frac{U^2}{L_P^2 R_L} \cdot \begin{pmatrix} M_{An}^2 + M_{Bn}^2 + M_{Cn}^2 + 2M_{An}M_{Bn}\cos\alpha \\ +2M_{An}M_{Cn}\cos\beta + 2M_{Bn}M_{Cn}\cos(\alpha-\beta) \end{pmatrix} \end{aligned} \tag{20}$$

According to (20), when $\cos\alpha = 1$, $\cos\beta = 1$ and $\cos(\alpha-\beta) = 1$, that is, when $\alpha = \beta = 0°$, the load receives the maximum power. The maximum received power is written as

$$P_{out\_n\_\max} = \frac{U^2}{L_P^2 R_L} \cdot (M_{An} + M_{Bn} + M_{Cn})^2 \tag{21}$$

According to (20) and (21), when the system parameters (U, L_P, R_L, α, β) are determined, the power received by the load is only related to the mutual inductance of the A, B and C phase coils at the location of the load. Furthermore, the maximum power received by the load is only related to the sum of the mutual inductance of the A, B and C coils at the position of the load, and has nothing to do with the number of loads. Compared with the S-S topology, this topology can ensure a constant current in the transmitting coil when the number of loads increases, thereby maintaining a constant received power of the load. Therefore, the three-phase LCC-S topology proposed in this paper solves the problem of power drop or surge when the load is accessed or removed under the S-S topology.

In addition, considering that three-dimensional WPT systems under multiple loads are mostly charged for similar devices, such as mobile phone display stands, their power requirements are basically the same. According to (21), when

the sum of the mutual inductance between the load and each transmitting coils are the same at any position of load, it can be guaranteed that each load receives the same power. Therefore, in the following analysis, we will optimize the coil based on the maximum power transmission of the load to achieve that each load receives the same power at the circumferential position, and when the load is charged with an angular shift, the power fluctuation caused by the load shift is reduced.

III. OPTIMAL DESIGN OF COILS IN TYPICAL MULTI-LOAD APPLICATION SCENARIOS

The Section II solves the problem of power fluctuation caused by the load moving in and out in the multi-load application scenario. However, when the load has an angular deviation, power fluctuations also occur in the load, which puts forward corresponding requirements for the optimal design of the transmitting coil. Therefore, this section will first introduce a typical application scenario, and optimize the structural layout of the transmitting coil based on this application scenario. In this way,, each load can receive the same maximum power, and when the load has an angular displacement, the problem of power fluctuation due to deviation of load is minimized as much as possible.

A. INTRODUCTION OF TYPICAL APPLICATION SCENARIOS

A typical application scenario of a multi-load three-dimensional omnidirectional WPT system is shown in Fig.6, which specifically includes a display stand, a transmitting coil, some typical receiving devices (mobile phones), a rail, and a slider. The transmitting coil is placed in the center of the display stand, and radiates a uniform electromagnetic field in the space. The rail is installed on the display surface, and a slider is placed on the track to fix the typical receiving device (mobile phone) and make the mobile phone face the center of the receiving coil. In addition, the slider can be moved as desired on the rail. When the customer removes the mobile phone from the slider to use the mobile phone, the mobile phone will stop charging, and when the mobile phone is returned to the slider, the mobile phone will continue to charge.

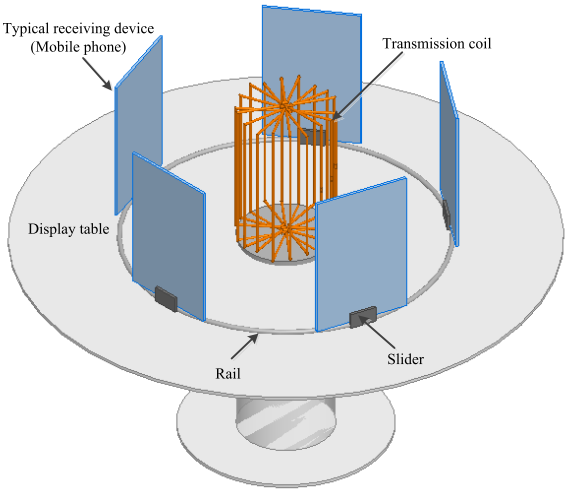

FIGURE 6. Typical application scenarios of multi-load three-dimensional omnidirectional WPT system.

B. OPTIMAL DESIGN OF TRANSMITTING COIL

Based on the requirements mentioned above, this part designed the single-phase coil structure as shown in Fig.7, with a difference of 60 degrees between each coil arms. The receiving coil uses the simplest rectangular coil. The top view of the single-phase transmitting coil and receiving coil is shown in Fig.8. d_1 is the transmission distance between the transceiver coil, d is the effective transmission distance, d and d_1 can be designed according to the actual application scenario, θ is the offset angle of the receiving coil, and the mutual inductance M between the primary and secondary coils varies with the offset angle of the receiving coil. However, according to the output power equation (21) in Section II, it can be known that the change in the mutual inductance M between the primary and secondary coils means the change in the received power of the load. Therefore, in this part, the mutual inductance model between the single-phase transmitting coil and the load is first established. Then, based on the change trend of mutual inductance varying with the offset angle θ, the structural layout of the transmitting coil is optimized to minimize the mutual inductance fluctuation of the load at the offset angle. Finally, the stability of load's receiving power under typical application scenarios is realized and each load receives the same amount of power at the maximum transmission power.

The mutual inductance M between the single-phase transmitting coil and the receiving coil can be calculated according

$$\begin{bmatrix} \dot{U}_A \\ \dot{U}_B \\ \dot{U}_C \\ 0 \\ \vdots \\ 0 \\ 0 \end{bmatrix} = \begin{bmatrix} j\omega L_{PA} & 0 & 0 & 0 & \cdots & 0 & 0 \\ 0 & j\omega L_{PB} & 0 & 0 & \cdots & 0 & 0 \\ 0 & 0 & j\omega L_{PC} & 0 & \cdots & 0 & 0 \\ j\omega M_{A1} & j\omega M_{B1} & j\omega M_{C1} & -R_L & \cdots & 0 & 0 \\ \vdots & \vdots & \vdots & \vdots & \ddots & \vdots & \vdots \\ j\omega M_{A(n-1)} & j\omega M_{B(n-1)} & j\omega M_{C(n-1)} & 0 & \cdots & -R_L & 0 \\ j\omega M_{An} & j\omega M_{Bn} & j\omega M_{Cn} & 0 & \cdots & 0 & -R_L \end{bmatrix} \begin{bmatrix} \dot{I}_A \\ \dot{I}_B \\ \dot{I}_C \\ \dot{I}_{S1} \\ \vdots \\ \dot{I}_{S(n-1)} \\ I_{Sn} \end{bmatrix} \tag{18}$$

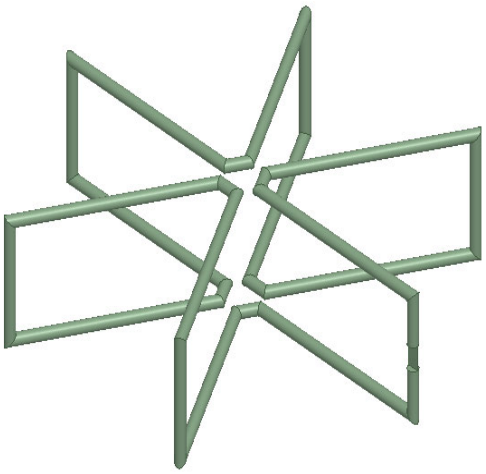

FIGURE 7. Single-phase transmitting coil structure diagram.

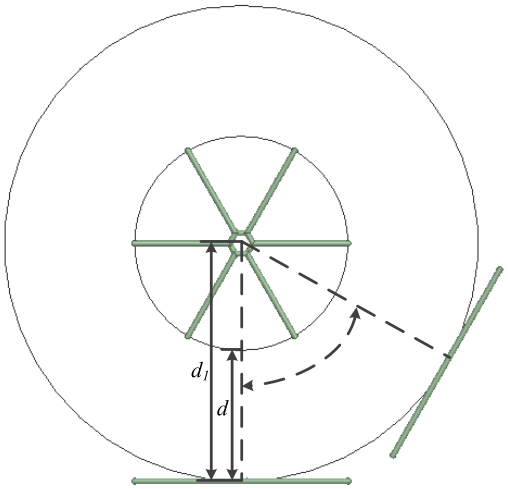

FIGURE 8. Top view of the relative position of the primary and secondary coils.

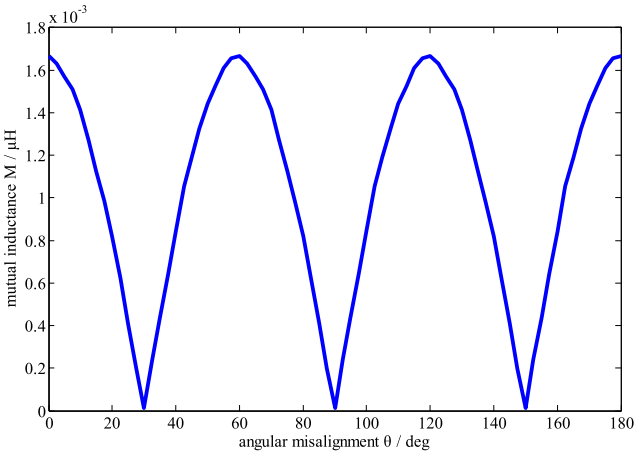

FIGURE 9. Tendency of mutual inductance varying with offset angle θ.

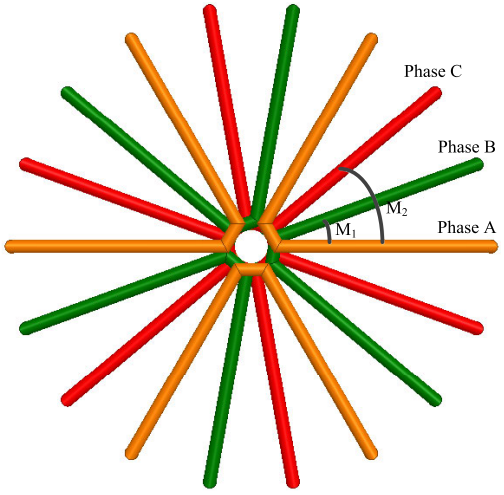

FIGURE 10. Schematic diagram of the relative position of the three-phase transmitting coil.

to the Neumann formula as

$$M = \frac{\mu_0 N_1 N_2}{4\pi} \oint\oint \frac{dl_1 \cdot dl_2}{r_{12}} \tag{22}$$

where N_1 and N_2 are the number of turns of a single-phase transmitting coil and a receiving coil respectively, l_1, l_2, dl_1 and dl_2 represent the length of the single-phase transmitting and receiving coils and their differentials, r_{12} is distance between dl_1 and dl_2, μ_0 is the vacuum permeability, and its value is $\mu_0 = 4\pi \times 10^{-7}$ H/m.

According to (22), when the offset angle θ is changed in the range of 0° to 180°, a trend of the mutual inductance between the single-phase transmitting coil and the receiver varying with the offset angle θ can be calculated. And it can be known from Fig.9 that the mutual induction period of the single-phase transmitting coil and the receiving coil is 60°, which is exactly consistent with the degrees between the bridge arms of the transmitting coil. This indicates that the period of the mutual inductance coincides with the period corresponding to the geometry of the transmitting coil. In addition, from the tendency of the mutual inductance between the single-phase transmitting coil and the receiving coil, when the receiving coil is perpendicular to the transmitting coil bridge arm, the mutual inductance M is zero, that is, there is a dead zone in the load receiving power, which is not conducive to achieving the same power for each load in a multi-load application scenario. At the same time, when the load has an angular displacement, it is not conducive to the stability of the received power.

Based on the tendency of mutual inductance between the above-mentioned single-phase transceiver coils and (21), it can be found that when the curve in Fig.9 is offset to a certain degree and the three mutual inductances are superimposed, the defect of zero load's receiving power can be compensated. The schematic diagram of the position of the three-phase transmitting coil is shown in Fig.10, where the same color indicates a coil, and m1 and m2 indicate the angle between the B-phase and C-phase coils and the A-phase coil,

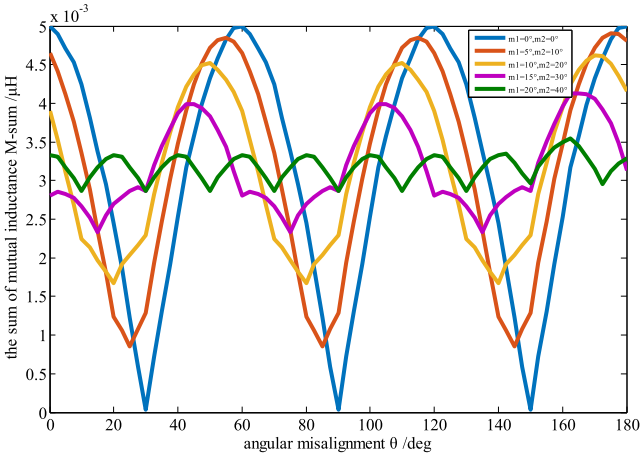

FIGURE 11. Tendency of the sum of the three mutual inductances varying with the offset angle θ.

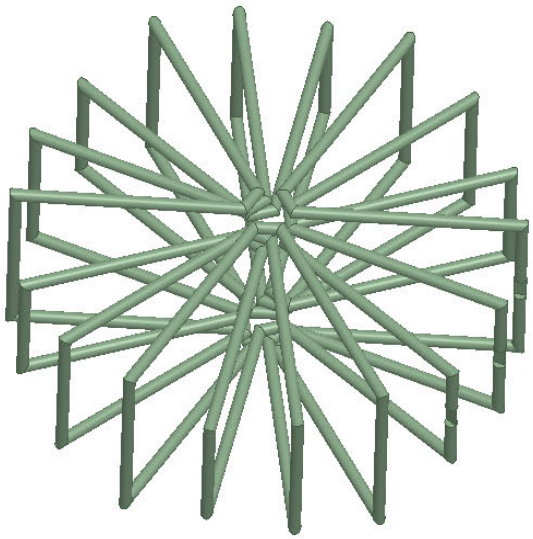

FIGURE 12. Schematic diagram of three-phase transmitting coil structure.

respectively. Therefore, based on the above-mentioned A-phase transmission coils, the curve of the sum of the three mutual inductances at different offset angles varying the offset angle can be drawn as shown in Fig.11.

In order to measure the power fluctuation of the load in the range of $0° \sim 180°$, the power fluctuation rate F is now defined as

$$F = \frac{P_{\max} - P_{\min}}{P_{\max}} = \frac{(M_{An} + M_{Bn} + M_{Cn})^2_{\max} - (M_{An} + M_{Bn} + M_{Cn})^2_{\min}}{(M_{An} + M_{Bn} + M_{Cn})^2_{\max}} \tag{23}$$

According to (23), the power fluctuation rate F of each phase transmitting coil at different offset positions can be calculated in Table 1

According to the above analysis, when the offset positions of the remaining two-phase transmitting coils are m1=20° and m2=40°, the load receiving power fluctuation rate is the smallest(about 24.87%), and the power fluctuation rate is reduced by 75.13%, which means that under this condition, the load can receive the same power and the degree of power fluctuation due to load offset can be reduced to a certain extent. Therefore, the structure of the three-phase transmitting coil shown in Fig.12 can be obtained by combining the relationship between the bridge arm of the single-phase transmitting coil and the mutual inductance. And the angle between the arms of the transmitting coils of each phase is 20 degrees. In summary, the three-phase transmitting coil structure of Fig.12 can greatly reduce the power fluctuations that occur when the load is shifted in position, and it can achieve multi-load same-power charging, which improves the practical significance of the three-phase omnidirectional WPT coil. Besides, it should be noted that the size of the three-phase transmitting coil can be large or small, depending on the actual application requirements.

Moreover, in addition to solving the problem of power fluctuations, the number of power supply is significantly reduced compared with previous studies after using the three-phase LCC-S topology and spatial orthogonal winding method proposed in this paper, and the specific comparison is shown in Table 2.

It can be seen from Table 2 that the LCC-S topology and winding method in this paper successfully reduced the three power supplies used in Literature [9]–[11] to one power supply, which greatly reduced the cost of power supply. Therefore, the system cost is greatly reduced, and the engineering application value of the three-phase omnidirectional WPT coil system is further improved.

IV. EXPERIMENTAL VERIFICATION

This part verifies the improvement of the proposed three-phase omnidirectional WPT system scheme on power stability. It is also verified that the proposed three-phase LCC-S topology can solve the problem of power drop or surge when the load is accessed or removed. The experimental results show that the system has basically no power fluctuation when the load is connected, and the power fluctuation problem caused by the load angle deviation is reduced, which effectively verifies the effectiveness and novelty of this scheme.

The experiment utilizes LCR meter 3522-50 LCR HiTESTER (HioKi E.E. Corporation, Nagano Prefecture, Japan) to measure the self-inductance of coils and mutual inductance between transmitting coils and receiving coil. The oscilloscope is adopted to measure the output voltage to calculate the output power which is used to verify the system power stability. In addition, the experiment also includes three-phase PWM wave input module consisting of DC voltage source, voltage regulator circuit module, DSP module and three-phase inverter circuit module, which produces the three-phase high frequency square wave. Furthermore,

TABLE 1. Power fluctuation rate *F* at different offset positions.

Offset position	Sum of maximum mutual inductance (nH)	Sum of minimum mutual inductance (nH)	Mutual inductance rate	Power volatility
m1=0°,m2=0°	5	0	100%	100%
m1=5°,m2=10°	4.846	0.8557	82.34%	96.88%
m1=10°,m2=20°	4.524	1.672	63.04%	86.34%
m1=15°,m2=30°	3.984	2.329	41.54%	65.82%
m1=20°,m2=40°	3.31	2.869	13.32%	24.87%

TABLE 2. The comparison of power supply type and quantity.

	Type of power supply	Quantity of power supplies
The traditional three-dimensional WPT system in the literature [9-11]	Current source	3
The three-phase WPT system proposed in this paper	voltage source	1

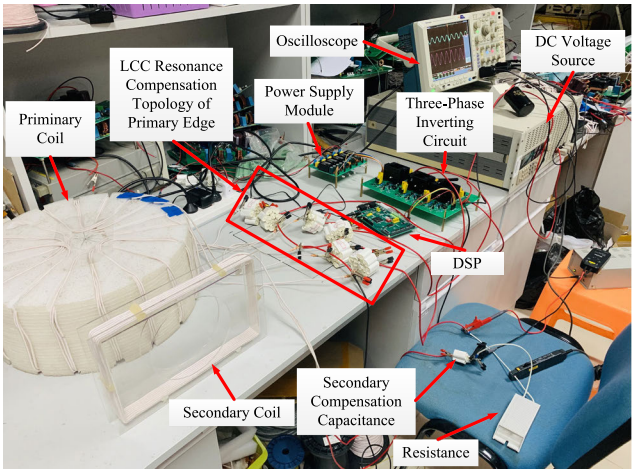

FIGURE 13. The complete experimental model and test system.

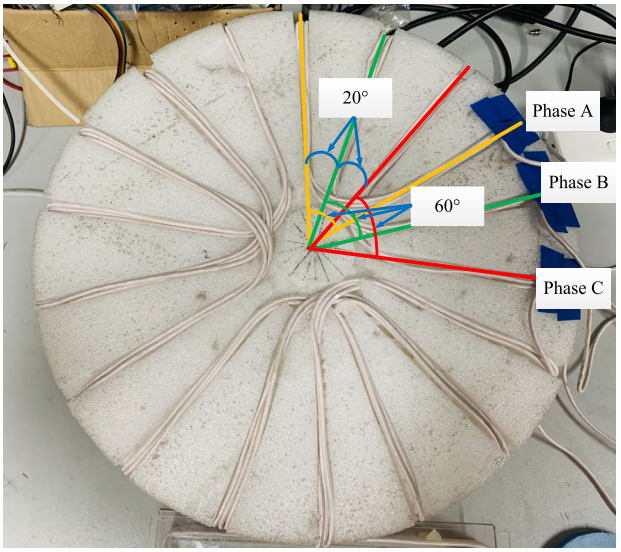

FIGURE 14. Three-phase transmitting coil model.

transceiver coils, compensation capacitors, compensation inductors, AC resistance loads and voltage detectors are also equipped. The complete experimental model and test system are shown in Fig.13.

In particular, the constructed three-phase transmitting coil model is consistent with the transmitting coil scheme proposed in the previous theoretical section as shown in Fig.14. The bridge arm angle between each phase coil is 60°, and the bridge arm angle between phases is 20°. Therefore, the basic measurement parameters of the entire experimental system are shown in Table 3. The operating frequency of the system is 85kHz, which is selected according to the internationally common SAE J2954 standard. Most wireless charging systems currently use this operating frequency [26].

Considering that the theoretical output power is maximum when the three-phase PWM waves are in phase, so the phase difference between the three-phase PWM waves set as zero in the experiment. Furthermore, in order to prevent the short circuit caused by the simultaneous conduction of the upper and lower bridge arms, the delay times of the rising and falling edges are set respectively. The waveform of the three-phase PWM wave driving circuit waveform is shown in Fig.15.

TABLE 3. Basic parameter values of experimental system.

Parameter	Value
Primary coil self-inductance of phase A (L_A)	17.377μH
Primary coil compensation capacitor of phase A (C_A)	0.405μF
Compensation self-inductance of phase A (L_{PA})	8.7361μH
Compensation capacitor of phase A (C_{PA})	0.401μF
Primary coil self-inductance of phase B (L_B)	17.534μH
Primary coil compensation capacitor of phase B (C_B)	0.403μF
Compensation self-inductance of phase B (L_{PB})	8.8706μH
Compensation capacitor of phase B (C_{PB})	0.395μF
Primary coil self-inductance of phase C (L_c)	16.915μH
Primary coil compensation capacitor of phase C (C_C)	0.426μF
Compensation self-inductance of phase C (L_{PC})	8.6867μH
Compensation capacitor of phase C (C_{PC})	0.403μF
Self-inductance of secondary coil 1 (L_{S1})	25.6μH

Waveforms of phase B also differ by 90 degrees, just because the time on the horizontal axis is different.

In order to verify that the proposed three-phase LCC-S topology can effectively solve the problem of power drop or surge when the load is accessed or removed. We add

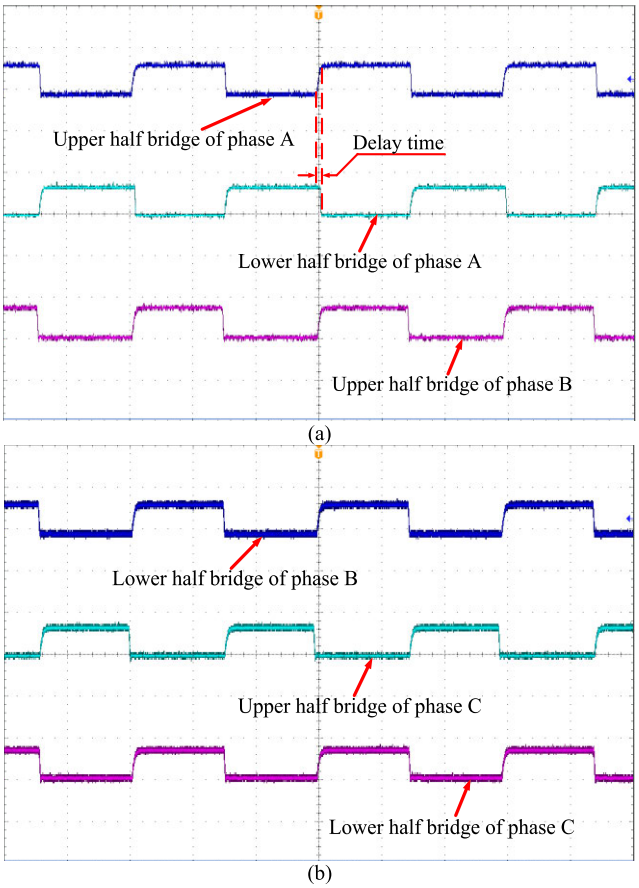

FIGURE 15. Three-phase PWM wave driving circuit waveform.

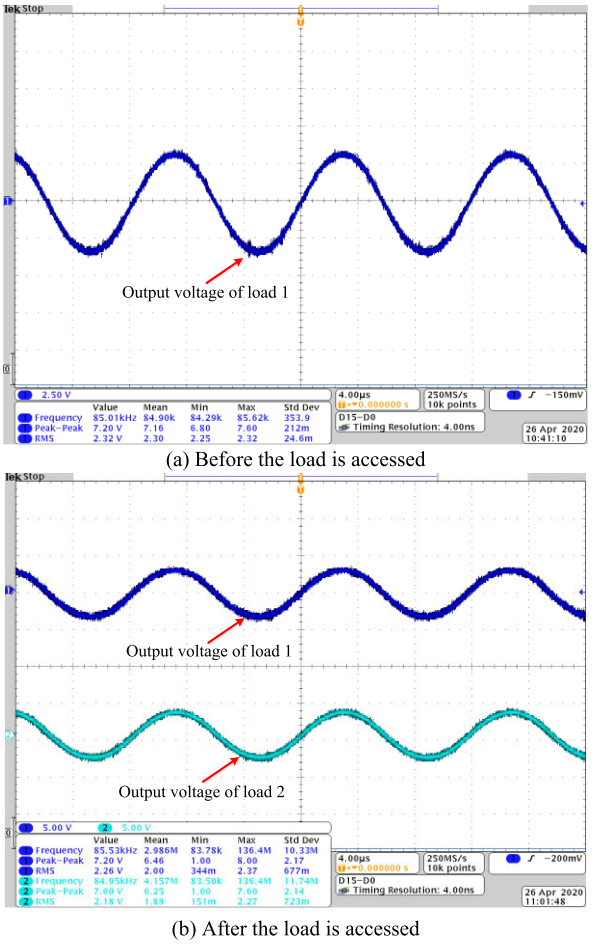

FIGURE 16. Voltage waveforms across the resistor before and after the load is accessed.

a set of loads to the working system, and use an oscilloscope to measure the load's voltage before and after the load is connected, as shown in Fig.16. It can be seen from Fig.16 that after the load is accessed, the load voltage changes from 241mV to 237mV, and almost no power drop occurs. Therefore, this solution can effectively solve the problem of power drop or surge caused by frequent load access or removal in multi-load scenarios.

In order to verify that the designed transmitting coil can effectively improve the power fluctuation problem of the load in the offset state, We firstly measure the mutual inductance of the receiving coils at different angles of the A-phase transmitting coils using the RLC measuring instrument. Since the period of the mutual inductance coincides with the period corresponding to the geometry of the transmitting coil (the period is 60 degrees), The trend of the mutual inductance varying with the offset angle can be measured in the range of $0 \sim 60$ degrees as shown in Fig.17(a). It is basically consistent with the theoretically calculated mutual inductance trend in Fig.17(b).

Then, we used an oscilloscope to measure the change trend of voltage value of load varying with the offset angle when the load offset angle changed in the range of 0° to 60° degrees, as shown in Fig.18(a). According to the calculation of $P=U^2/R_L$, the trend of the received power of the load varying with the offset angle is shown in Fig.18(b). According to Fig.18, when the offset angle is 30°, the voltage value and the received power value of the load are the largest, which are 2.36V and 5.57W respectively. When the offset angle is 0°, the voltage value and the received power value of the load are the smallest, which are 2.01V and 4.04W respectively.

According to (23), it can be calculated that the power fluctuation rate of this system is about 27.46%, and compared with the theoretical value of 24.87%, the power fluctuation is slightly increased by 2.59% which is within the acceptable range. This phenomenon may be due to the incomplete alignment of the transmitting and receiving coils when the load is shifted along its own central axis during the movement process. However, this incomplete alignment will hardly occur in practical applications, because the load is located on the slider and the slider can only move along the track, which make the load plane and the transmitting coil always face each other during the movement. It can be seen that compared with the previous scheme, the scheme has a significant improvement in power stability, and the power has been increased by about 72.54%, which further proves the effectiveness and practicability of the scheme.

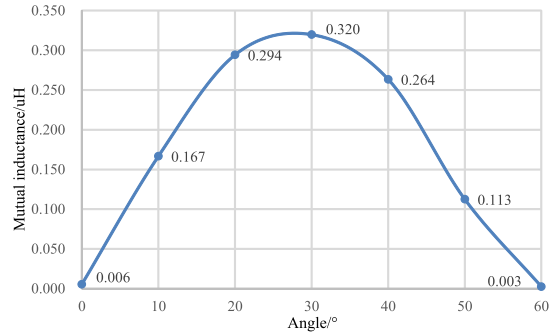

(a) Measured value

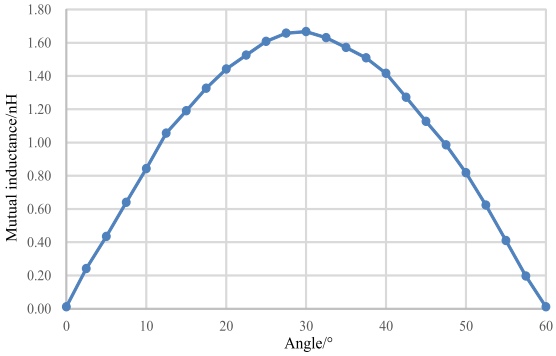

(b) Calculated value

FIGURE 17. **Variation trend of A-phase mutual inductance varying with offset angle in one bridge arm period.**

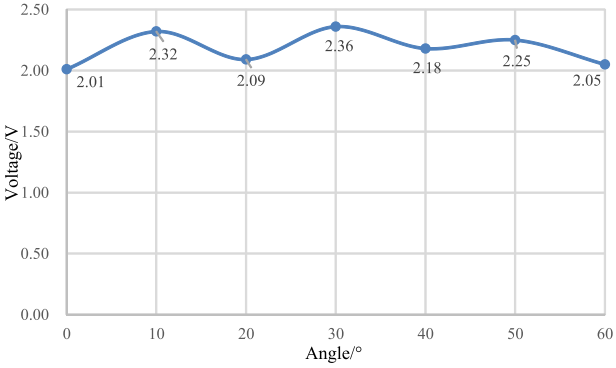

(a) Trend of Load voltage varying with offset angle

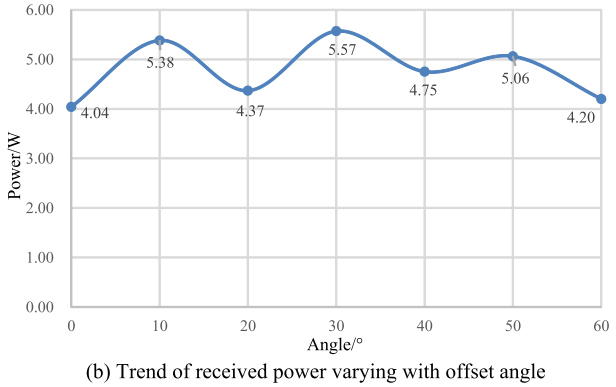

(b) Trend of received power varying with offset angle

FIGURE 18. **Trend of load voltage and receiving power varying with offset angle.**

V. CONCLUSIONS

This paper proposes a novel three-phase WPT system, which combines the LCC-S topology with three-phase circuits to solve the problem of power drop or sudden rise when the load is accessed or removed in a multi-load application scenario. Based on this, a three-phase omnidirectional WPT system coil scheme is proposed, which solves the problem of power fluctuation when the load's angle is shifted, and further improves the stability of the transmitted power. Firstly, the power characteristics of the resonant compensation topology and the power stability of the system are analyzed based on the mutual inductance equivalent theory. We conclude that the three-phase LCC-S topology is more suitable for multi-load application scenarios. It is verified through theory and experiments that the three-phase LCC-S topology can solve the power fluctuation problem when the load is accessed or removed. Subsequently, the influence of the three-phase transmitting coil structure on the power stability of the system is analyzed based on the three-phase LCC-S topology, and the optimal coil scheme of the three-phase omnidirectional WPT system is obtained based on the analysis of the mutual inductance variation trend, that is, when the bridge arms of the three-phase transmitting coil are 20 ° apart from each other, the system power fluctuation is the smallest. Compared with the original scheme, the theoretical calculation results show that the optimized coil scheme reduces the power fluctuation rate by 75.13%. The experimental results show that the optimized coil reduces the power fluctuation rate by 72.54%, and the theoretical analysis is basically consistent with the experiment, which represents the feasibility of the proposed coil scheme. In summary, the proposed three-phase WPT system coil optimization scheme combined with the three-phase LCC-S topology can effectively solve the problem of power fluctuations when the load is accessed or removed and the load is shifted, which improve the stability of system transmission power.

REFERENCES

[1] S. Y. R. Hui, W. Zhong, and C. K. Lee, "A critical review of recent progress in mid-range wireless power transfer," *IEEE Trans. Power Electron.*, vol. 29, no. 9, pp. 4500–4511, Sep. 2014.

[2] S. Li and C. Chris Mi, "Wireless power transfer for electric vehicle applications," *IEEE J. Emerg. Sel. Topics Power Electron.*, vol. 3, no. 1, pp. 4–17, Mar. 2015.

[3] H. A. Fadhil, S. G. Abdulqader, and S. A. Aljunid, "Implementation of wireless power transfer system for smart home applications," in *Proc. IEEE 8th GCC Conf. Exhib.*, Feb. 2015, pp. 1–4.

[4] R. Jegadeesan, Y. X. Guo, and M. Je, "Electric near-field coupling for wireless power transfer in biomedical applications," in *IEEE MTT-S Int. Microw. Symp. Dig.*, Dec. 2013, pp. 1–3.

[5] Y. Zhang, T. Lu, Z. Zhao, K. Chen, F. He, and L. Yuan, "Wireless power transfer to multiple loads over various distances using relay resonators," *IEEE Microw. Wireless Compon. Lett.*, vol. 25, no. 5, pp. 337–339, May 2015.

[6] K. Lee and D.-H. Cho, "Analysis of wireless power transfer for adjustable power distribution among multiple receivers," *IEEE Antennas Wireless Propag. Lett.*, vol. 14, pp. 950–953, 2015.

[7] B. L. Cannon, J. F. Hoburg, D. D. Stancil, and S. C. Goldstein, "Magnetic resonant coupling as a potential means for wireless power transfer to multiple small receivers," *IEEE Trans. Power Electron.*, vol. 24, no. 7, pp. 1819–1825, Jul. 2009.

[8] M. Fu, T. Zhang, C. Ma, and X. Zhu, "Efficiency and optimal loads analysis for multiple-receiver wireless power transfer systems," *IEEE Trans. Microw. Theory Techn.*, vol. 63, no. 3, pp. 801–812, Mar. 2015.

[9] W. M. Ng, C. Zhang, D. Lin, and S. Y. Ron Hui, "Two- and three-dimensional omnidirectional wireless power transfer," *IEEE Trans. Power Electron.*, vol. 29, no. 9, pp. 4470–4474, Sep. 2014.
[10] D. Lin, C. Zhang, and S. Y. R. Hui, "Mathematical analysis of omnidirectional wireless power Transfer—Part-I: Two-dimensional systems," *IEEE Trans. Power Electron.*, vol. 32, no. 1, pp. 625–633, Jan. 2017.
[11] D. Lin, C. Zhang, and S. Y. R. Hui, "Mathematic analysis of omnidirectional wireless power Transfer—Part-II three-dimensional systems," *IEEE Trans. Power Electron.*, vol. 32, no. 1, pp. 613–624, Jan. 2017.
[12] C. Zhang, D. Lin, and S. Y. Hui, "Basic control principles of Omnidirectional wireless power transfer," *IEEE Trans. Power Electron.*, vol. 31, no. 7, pp. 5215–5227, Jul. 2016.
[13] C. Jiang, F. Liu, X. Ruan, and X. Chen, "Transmission characteristics analysis of a three-phase magnetically coupled resonant wireless power transfer system," in *Proc. IEEE Energy Convers. Congr. Expo. (ECCE)*, Sep. 2016, pp. 1–6.
[14] X. L. Chen, X. W. Fu, and C. Jiang, "Magnetic-field-model and circuit-model based analysis of three-phase magnetically coupled resonant wireless power transfer systems with cylinder-shaped coils," *J. Power Electron.*, vol. 18, no. 4, pp. 1154–1164, Jul. 2018.
[15] N. Ha-Van and C. Seo, "Analytical and experimental investigations of omnidirectional wireless power transfer using a cubic transmitter," *IEEE Trans. Ind. Electron.*, vol. 65, no. 2, pp. 1358–1366, Feb. 2018.
[16] H. Wang, L. Deng, H. Luo, H. Zhao, S. Huang, J. Xiao, and C. Liao, "Omnidirectional magnetic resonant coupling wireless power transfer system with a cubic spiral transmitter," *AIP Adv.*, vol. 9, no. 6, Jun. 2019, Art. no. 065211.
[17] Z. Zhang, B. Zhang, and J. Wang, "Optimal design of quadrature-shaped pickup for omnidirectional wireless power transfer," *IEEE Trans. Magn.*, vol. 54, no. 11, pp. 1–5, Nov. 2018.
[18] Z. Zhang and B. Zhang, "Angular-misalignment insensitive omnidirectional wireless power transfer," *IEEE Trans. Ind. Electron.*, vol. 67, no. 4, pp. 2755–2764, Apr. 2020.
[19] J. Feng, Q. Li, and F. C. Lee, "Coil and circuit design of omnidirectional wireless power transfer system for portable device application," in *Proc. IEEE Energy Convers. Congr. Expo. (ECCE)*, Portland, OR, USA, Sep. 2018, pp. 914–920.
[20] W. Han, K. T. Chau, C. Jiang, W. Liu, and W. H. Lam, "Design and analysis of quasi-omnidirectional dynamic wireless power transfer for Fly-and-Charge," *IEEE Trans. Magn.*, vol. 55, no. 7, pp. 1–9, Jul. 2019.
[21] M. J. Chabalko and A. P. Sample, "Three-dimensional charging via multimode resonant cavity enabled wireless power transfer," *IEEE Trans. Power Electron.*, vol. 30, no. 11, pp. 6163–6173, Nov. 2015.
[22] J. Feng, Q. Li, F. C. Lee, and M. Fu, "Transmitter coils design for free-positioning omnidirectional wireless power transfer system," *IEEE Trans. Ind. Informat.*, vol. 15, no. 8, pp. 4656–4664, Aug. 2019.
[23] F. Liu, Z. Ding, X. Fu, and R. M. Kennel, "Parametric optimization of a three-phase MCR WPT system with cylinder-shaped coils oriented by soft-switching range and stable output power," *IEEE Trans. Power Electron.*, vol. 35, no. 1, pp. 1036–1044, Jan. 2020.
[24] C. Zhong, B. Luo, F. Ning, and W. Liu, "Reactance compensation method to eliminate cross coupling for two-receiver wireless power transfer system," *IEICE Electron. Exp.*, vol. 12, no. 7, 2015, Art. no. 20150016.
[25] L. Tan, S. Pan, and C. Xu, "Study of constant current-constant voltage output wireless charging system based on compound topologies," *J. Power Electron.*, vol. 17, no. 4, pp. 1109–1116, Jul. 2017.
[26] J. Schneider, *Wireless Power Transfer for Light-Duty Plug-In/Electric Vehicles and Alignment Methodology*, 2rd ed. Warrendale, PA, USA: SAE International, 2017, pp. 99–156.

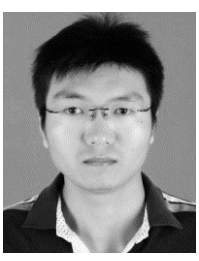

LINLIN TAN received the B.S. degree in electrical engineering and automation from Harbin Engineering University, Harbin, China, in 2008, and the Ph.D. degree in electrical engineering from Southeast University, Nanjing, China, in 2014. He is currently working as a Lecturer with the School of Electrical Engineering, Southeast University. He has published more than 20 articles. His current research interests include wireless power transfer, wireless charging for electric vehicles, and wireless V2G.

RUYING ZHONG received the B.S. degree from the School of Electrical Engineering and Automation, Nanjing Normal University, Nanjing, China, in 2018. She is currently pursuing the master's degree with the School of Electrical Engineering, Southeast University, Nanjing. Her current research interest includes wireless power transfer.

ZONGYAO TANG received the B.S. degree from the College of Electrical Engineering, Nanjing University of Aeronautics and Astronautics, Nanjing, China, in 2017. He is currently pursuing the master's degree with the School of Electrical Engineering, Southeast University, Nanjing. His current research interests include wireless power transfer, wireless charging coil, and system optimization.

TIANYI HUANG received the B.S. degree from the College of Electrical Engineering, Nanjing Institute of Technology, Nanjing, China, in 2018. He is currently pursuing the master's degree with the School of Electrical Engineering, Southeast University, Nanjing. His current research interests include wireless power transfer and advanced power semiconductors.

XUELIANG HUANG (Member, IEEE) received the B.S., M.S., and Ph.D. degrees in electrical engineering from Southeast University, Nanjing, China, in 1991, 1994, and 1997, respectively.

From 2002 to 2004, he worked with the University of Tokyo, as a Postdoctoral Researcher, where he was a also Postdoctoral Researcher, From 2002 to 2004. Since 2004, he has been a Professor with the Electrical Engineering Department, Southeast University. He is the author of four books, more than 150 articles and more than 40 inventions, and holds one PCT patent. His research interests include novel wireless power transfer systems, analysis of electromagnetic field, applied electromagnetics, and intelligent electricity technology. He received the Teaching Achievement Prize of Jiangsu Province, in 2009, and the Ministry of Environmental Protection Science and Technology Prize, in 2012. He is the Editor of the journal Transactions of China Electrotechnical Society.

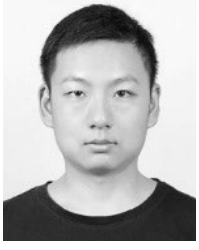

TAO MENG received the B.S. degree from the College of Electrical Engineering, Shanghai University of Electric Power, Shanghai, China, in 2018. He is currently pursuing the master's degree with the School of Electrical Engineering, Southeast University, Nanjing, China. His current research interests include wireless power transfer and magnetic coupling mechanism.

XUEFENG ZHAI, photograph and biography not available at the time of publication.

CHENGLIANG WANG, photograph and biography not available at the time of publication.

YAN XU, photograph and biography not available at the time of publication.

QINGSHENG YANG, photograph and biography not available at the time of publication.